Rapid Communications

High-T_c superconductivity up to 55 K under high pressure in a heavily electron doped $Li_{0.36}(NH_3)_yFe_2Se_2$ single crystal

P. Shahi,[1,2] J. P. Sun,[1,2] S. H. Wang,[3] Y. Y. Jiao,[1,2] K. Y. Chen,[1,2] S. S. Sun,[3] H. C. Lei,[3,*] Y. Uwatoko,[4] B. S. Wang,[1,2] and J.-G. Cheng[1,2,†]

[1]*Beijing National Laboratory for Condensed Matter Physics and Institute of Physics, Chinese Academy of Sciences, Beijing 100190, China*

[2]*School of Physical Sciences, University of Chinese Academy of Sciences, Beijing 100190, China*

[3]*Department of Physics, Beijing Key Laboratory of Opto-electronic Functional Materials & Micro-nano Devices, Renmin University of China, Beijing 100872, China*

[4]*Institute for Solid State Physics, University of Tokyo, 5-1-5 Kashiwanoha, Kashiwa, Chiba 277-8581, Japan*

(Received 25 September 2017; revised manuscript received 7 January 2018; published 22 January 2018)

We report a high-pressure study on the heavily electron doped $Li_{0.36}(NH_3)_yFe_2Se_2$ single crystal by using a cubic anvil cell apparatus. The superconducting transition temperature $T_c \approx 44$ K at ambient pressure is first suppressed to below 20 K upon increasing pressure to $P_c \approx 2$ GPa, above which the pressure dependence of $T_c(P)$ reverses and T_c increases steadily to ca. 55 K at 11 GPa. These results thus evidence a pressure-induced second high-T_c superconducting (SC-II) phase in $Li_{0.36}(NH_3)_yFe_2Se_2$ with the highest $T_c^{max} \approx 55$ K among the FeSe-based bulk materials. Hall data confirms that in the emergent SC-II phase the dominant electron-type carrier density undergoes a fourfold enhancement and tracks the same trend as $T_c(P)$. Interestingly, we find a nearly parallel scaling behavior between T_c and the inverse Hall coefficient for the SC-II phases of both $Li_{0.36}(NH_3)_yFe_2Se_2$ and (Li,Fe)OHFeSe. The present study demonstrates that high pressure offers a distinctive means to further raise the maximum T_c of heavily electron doped FeSe-based materials by increasing the effective charge-carrier concentration via a possible Fermi-surface reconstruction at P_c.

DOI: 10.1103/PhysRevB.97.020508

To find out the approaches to raise the critical temperature T_c of unconventional superconductors is one of the most enduring problems in contemporary condensed-matter physics. The great tunability of T_c for bulk FeSe from 8 K to over 40 K [1–7] and the possible high T_c exceeding 100 K in the monolayer $FeSe/SrTiO_3$ [8,9] have spurred tremendous interest recently. The principal route to raise the T_c of FeSe is to dope electron, which has been successfully achieved via the interlayer intercalations [$A_xFe_{2-y}Se_2$ (A = K, Rb, ...), $A_x(NH_3)_yFe_2Se_2$, and (Li,Fe)OHFeSe] [2,3,7,10,11], interface charge transfer [8], surface K dosing [12,13], and gate-voltage regulation [6,14]. A common Fermi-surface topology consisting of electron pockets only has been confirmed by the angle-resolved photoemission spectroscopy (ARPES) measurements on these heavily electron doped (HED) FeSe derivatives [15–17]. Based on the bulk resistivity measurements on these HED FeSe bulk materials, the highest T_c at ambient pressure, i.e., $T_c^{onset} = 46.6$ K and $T_c^{zero} = 44.8$ K, was achieved in the FeSe flake in a field-effect transistor device based on a solid ion conductor [14]. Further enhancement of T_c via adding more electrons seems to be plagued by the observed insulating state in the overdoped regime [14,18,19]. Whether the T_c of HED FeSe bulk materials can reach well above 50 K or even approach that of monolayer $FeSe/SrTiO_3$ remains an open issue.

Given the limitations of electron doping, it is imperative to explore other routes to further enhance T_c of these HED FeSe materials. The application of high pressure can provide an alternative means. It was reported that pressurization on $A_xFe_{2-y}Se_2$ [20,21] and $Cs_{0.4}(NH_3)_yFeSe$ [22] can first reduce T_c and then above a critical pressure P_c induce a second high-T_c superconducting phase (denoted as SC-II to distinguish from the ambient pressure SC-I phase). The observed T_c of SC-II is ca. 10 K higher than that of SC-I. Our recent high-pressure study on (Li,Fe)OHFeSe also evidenced such an SC-II phase above $P_c \approx 5$ GPa, reaching a record high $T_c^{onset} = 51$ K and $T_c^{zero} = 46.5$ K at 12.5 GPa [23]. More intriguingly, we observed a sharp transition of the normal state from Fermi liquid for SC-I to non-Fermi liquid for SC-II in (Li,Fe)OHFeSe. In addition, the emergence of SC-II is accompanied by a concurrent enhancement of electron carrier density. These observations demonstrated that high pressure can play a very distinctive role to tune the normal and superconducting properties of these HED FeSe materials.

In order to avoid the complications from the magnetism of intercalated (Li,Fe)OH layer in (Li,Fe)OHFeSe [3], we turn our attention to the recently synthesized $Li_{0.36}(NH_3)_yFe_2Se_2$ single crystal [24], which can reach an optimal $T_c^{onset} \approx 44.3$ K at ambient pressure. By performing magnetotransport measurements up to 12 GPa, we find that the SC-I phase is quickly suppressed under a low $P_c \approx 2$ GPa, above which an SC-II phase emerges and the highest T_c^{onset} reaches ca. 55 K at $P \geqslant 10$ GPa. Similar to (Li,Fe)OHFeSe [23], the reemergence of SC-II is also accompanied with a concurrent enhancement of electron carrier density. Importantly, we obtain a linear relationship between T_c and the inverse Hall coefficient for the SC-II phases of both systems. In this Rapid Communication,

*hlei@ruc.edu.cn
†jgcheng@iphy.ac.cn

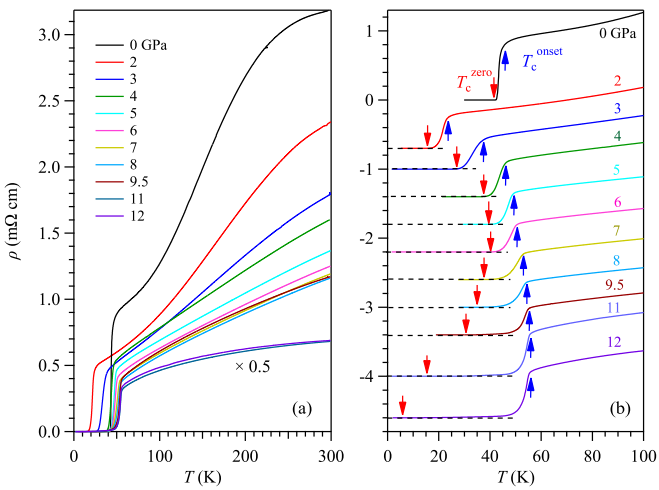

FIG. 1. High-pressure resistivity $\rho(T)$ for a $Li_{0.36}(NH_3)_yFe_2Se_2$ single crystal. (a) $\rho(T)$ curves in the whole temperature range illustrating the overall behaviors under pressure up to 12 GPa. At 11 and 12 GPa, the $\rho(T)$ curves were scaled by a factor of 0.5. (b) $\rho(T)$ curves below 100 K illustrating the variation of the superconducting transition temperatures with pressure. Except for data at 0 GPa, all other curves in (b) have been vertically shifted for clarity. The onset T_c^{onset} (up-pointing arrow) was determined as the temperature where $\rho(T)$ curves above and below intersect with each other, whereas the T_c^{zero} (down-pointing arrow) was determined as the zero-resistivity temperature.

we demonstrate a way for high pressure to further raise T_c of these HED FeSe materials via increasing effective electron carrier density.

Details about the crystal growth and characterizations of $Li_{0.36}(NH_3)_yFe_2Se_2$ single crystal at ambient pressure can be found elsewhere [24]. Each unit cell consists of two FeSe layers with lattice parameters $a = 3.7704$ and $c = 16.973$ Å in the space-group *I4/mmm* (No. 139). The chemical composition was determined via inductively coupled plasma atomic emission spectroscopy and energy-dispersive x-ray spectroscopy measurements [24]. Because the NH_3 molecules are neutral and will not transfer electron carriers into FeSe layers, they should not affect the physical properties of the $Li_{0.36}(NH_3)_yFe_2Se_2$ single crystal.

A palm cubic anvil cell (CAC) apparatus was employed for the accurate measurements of magnetotransport and ac magnetic susceptibility under hydrostatic pressures up to 12 GPa [25]. The standard four-probe method was used for the resistivity measurement, and the current is applied within the *ab* plane with the magnetic field along the *c* axis. An antisymmetrized (symmetrized) method was performed to get the $\rho_{xy}(H)$ and $\rho_{xx}(H)$ data. The mutual induction method was employed for the ac magnetic susceptibility measurements with an excitation current of 1 mA and 317 Hz. The superconducting shielding volume fraction was estimated by comparing with the superconducting signal of Pb. Glycerol was used as the pressure transmitting medium, and the pressure values inside the CAC were calibrated at room temperature by measuring the characteristic transitions of bismuth and lead from resistivity.

Figure 1(a) shows the resistivity $\rho(T)$ under various pressures up to 12 GPa in the whole temperature range for $Li_{0.36}(NH_3)_yFe_2Se_2$. Here, we determine T_c^{zero} as the zero-resistivity temperature and define the onset T_c^{onset} as the temperature where $\rho(T)$ above and below intersect with each other. At ambient pressure, $\rho(T)$ displays a broad hump centered around 220 K and shows a sharp superconducting transition with $T_c^{\text{onset}} = 44.3$ K and $T_c^{\text{zero}} = 42$ K, in agreement with the previous report [24]. The normal-state $\rho(T)$ decreases considerably, and the hump feature fades away gradually with increasing pressure to 3 GPa, above which a quasilinear behavior is restored in a broad temperature range. Similar behavior has also been observed in (Li,Fe)OHFeSe [23]. As illustrated in Fig. 1(a), $\rho(T)$ at $P > 10$ GPa exhibits an anomalous bendover in the normal state. As discussed below, such a behavior should be attributed to the partial conversion of $Li_{0.36}(NH_3)_yFe_2Se_2$ to pristine FeSe, which transforms to three-dimensional MnP-type structure with a semiconducting behavior above 10 GPa [26].

At low temperatures, the superconducting transition displays a nonmonotonic variation with pressure, which can be seen more clearly in Fig. 1(b) from the vertically shifted $\rho(T)$ curves below 100 K. Pressure first reduces T_c quickly to $T_c^{\text{onset}} = 25$ K and $T_c^{\text{zero}} = 15$ K at 2 GPa. Interestingly, the pressure dependence of $T_c(P)$ suddenly reverses at $P > 2$ GPa and T_c^{onset} (T_c^{zero}) increases to 37 K (26 K) at 3 GPa, thus *evidencing the emergence of SC-II* as seen in (Li,Fe)OHFeSe [23]. But the critical pressure of $P_c \approx 2$ GPa is lower than that of (Li,Fe)OHFeSe. As illustrated in Fig. 1(b), T_c^{onset} and T_c^{zero} exhibit distinct pressure dependences at $P > 2$ GPa: T_c^{onset} first increases quickly with pressure to ~50 K at 6 GPa and then levels off reaching the highest 55 K at 11 GPa and finally decreases slightly with pressure; in contrast, T_c^{zero} first tracks T_c^{onset} and reaches the maximum value of ~40 K at 6 GPa and then decreases quickly with the difference between T_c^{onset} and T_c^{zero} enlarged considerably at $P > 6$ GPa. Eventually, T_c^{zero} can be barely reached at 11 and 12 GPa despite a high $T_c^{\text{onset}} \approx 55$ K. Since our previous studies have demonstrated an excellent hydrostatic pressure condition up to 15 GPa for CAC [25], the observed discrepancy between T_c^{onset} and T_c^{zero} above 6 GPa reflects an intrinsic pressure response of $Li_{0.36}(NH_3)_yFe_2Se_2$, implying that the superconducting transition either consists of a distribution of different T_c's or is not bulk in nature.

To further track the evolutions of $T_c(P)$ and to investigate the nature of broad superconducting transitions above 6 GPa, we measured ac magnetic susceptibility $4\pi\chi(T)$ up to 11 GPa. As shown in Fig. 2(a) for $P < 6$ GPa, a single superconducting diamagnetic drop can be clearly observed below T_c^{χ}, which increases with pressure in perfect agreement with the $\rho(T)$ data. In addition, the superconducting shielding volume fraction increases with pressure and reaches ~90% at 5 GPa, signaling a bulk nature for the observed SC-II at $P \leqslant 6$ GPa. In contrast, the $4\pi\chi(T)$ curves at 7 and 9 GPa, Fig. 2(b), evidence two superconducting transitions as indicated by the two successive drops, which correspond to the T_c^{onset} and T_c^{zero} determined from $\rho(T)$. The superconducting phase with a higher $T_c \sim 50$ K can attain a volume fraction of ca. 30% and induces the sudden drop in resistivity at T_c^{onset}, but the sample can reach zero resistivity only when the lower-T_c phase also enters the superconducting state below ~33 K. Although the higher T_c phase remains nearly unchanged with pressure, both T_c and

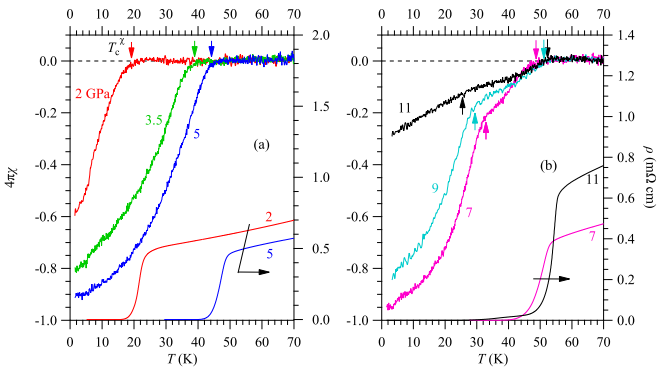

FIG. 2. The ac magnetic susceptibility $4\pi\chi(T)$ curves and resistivity $\rho(T)$ curves measured under different pressures up to 11 GPa. (a) The superconducting diamagnetic signal $4\pi\chi(T)$ and $\rho(T)$ below 5 GPa, and T_c^{χ} is in agreement with zero resistivity. (b) The superconducting diamagnetic signal $4\pi\chi(T)$ and $\rho(T)$ up to 11 GPa. The two transitions are marked by arrows and are in agreement with zero resistivity and the onset of the superconductivity.

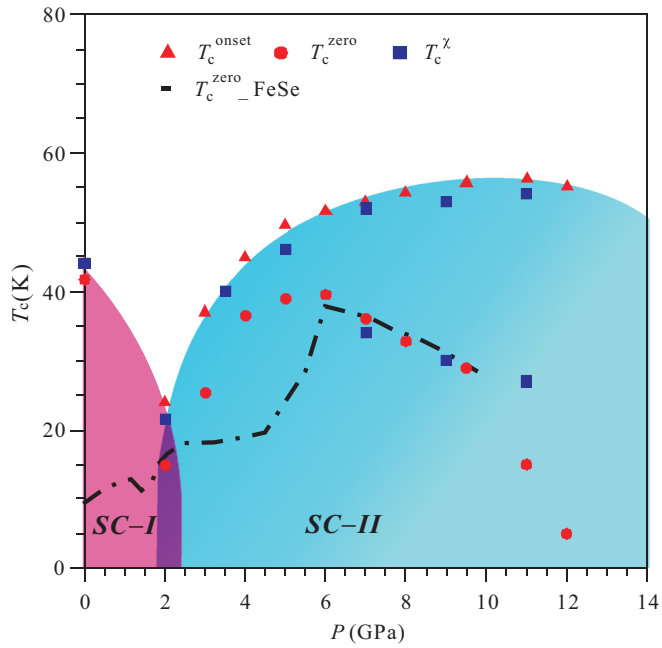

FIG. 3. The T-P phase diagram of the $Li_{0.36}(NH_3)_yFe_2Se_2$ single crystal. The pressure dependence of the superconducting transition temperatures T_cs up to 12 GPa. The values of T_c^{onset}, T_c^{zero}, and T_c^{χ} are determined from the high-pressure resistivity and ac magnetic susceptibility shown in Figs. 1 and 2. The T_c^{zero} of the FeSe single crystal is taken from Ref. [26].

the volume fraction of the lower-T_c phase decrease and nearly vanish at 11 GPa. As such, $\rho(T)$ at 11 GPa can hardly reach zero until very low temperatures.

From these above characterizations, we can conclude that the SC-II phase is bulk in nature for $P \leqslant 6$ GPa, whereas the sample contains two superconducting phases with different T_c's above 6 GPa: The high-T_c ($\geqslant$50 K) phase has a small but nearly constant volume fraction ~30% to 11 GPa, whereas the low-T_c ($\leqslant$33 K) phase shrinks and vanishes completely above 11 GPa. Figure 3 summarizes the pressure dependences of T_c^{onset}, T_c^{zero}, and T_c^{χ} for $Li_{0.36}(NH_3)_yFe_2Se_2$ together with the T_c^{zero} of FeSe for comparison [26]. Since the obtained T_c^{χ} of the low-T_c phase and the T_c^{zero} from $\rho(T)$ at $P \geqslant 6$ GPa match perfectly with the T_c^{zero} of FeSe, it is likely that $Li_{0.36}(NH_3)_yFe_2Se_2$ has been partially converted to the pristine FeSe due to the extrusion of Li^+ and ammonia, which might be associated with the solidification of the pressure transmitting medium, glycerol, at about 6 GPa at room temperature [27]. Such a speculation is supported by the disappearance of low-T_c phase at 11 GPa when the pristine layered FeSe transforms to the MnP-type structure with a semiconducting behavior [26]. The presence of semiconducting FeSe above 10 GPa can also explain the observed bendover in the $\rho(T)$ curves of 11 and 12 GPa, Fig. 1(a). Nevertheless, the smooth evolution of T_c^{onset} and T_c^{χ} of the high-T_c phase at $P > 6$ GPa should reflect the intrinsic pressure responses for the remaining pressure-induced SC-II phase. Below we thus focus on the variations of T_c^{onset} and T_c^{χ} as a function of pressure for $Li_{0.36}(NH_3)_yFe_2Se_2$.

The temperature-pressure phase diagram shown in Fig. 3 depicts explicitly the evolution of the superconducting phases of $Li_{0.36}(NH_3)_yFe_2Se_2$ under pressure. The high-T_c SC-I phase, initially achieved at ambient pressure via doping electrons through inserting Li^+ and ammonia in between the FeSe layers, is quickly suppressed by pressure, and the SC-II phase emerges above $P_c \approx 2$ GPa and exists in a broad pressure range. The pressure-induced SC-II in $Li_{0.36}(NH_3)_yFe_2Se_2$ resembles those observed in $A_xFe_{2-y}Se_2$ [20,21], $Cs_{0.4}(NH_3)_yFeSe$ [22], and $(Li_{1-x}Fe_x)OHFeSe$ [23], pointing to a universal phenomenon for these HED FeSe materials under pressure. But, some specific features for $Li_{0.36}(NH_3)_yFe_2Se_2$ are noteworthy; i.e., the $P_c \approx 2$ GPa for the emergence of SC-II is the lowest whereas the maximum $T_c^{onset} \approx 55$ K is the highest among the studied HED FeSe-derived materials. For comparison, the P_c and the maximum T_c^{onset} are 5 GPa, 51 K for $(Li_{1-x}Fe_x)OHFeSe$ [23] and 10 GPa, 49 K for $A_xFe_{2-y}Se_2$ [20], respectively. It seems that P_c depends on the bonding strength between FeSe and the intercalated layer; the weakest bonding in $Li_{0.36}(NH_3)_yFe_2Se_2$ gives rise to the lowest P_c. On the other hand, the maximum T_c achievable in the SC-II phase seems to be proportional to the initial T_c or the electron doping level at ambient pressure. The maximum $T_c^{onset} \approx 55$ K in $Li_{0.36}(NH_3)_yFe_2Se_2$ is very close to the highest T_c achieved in the FeAs-based materials [28].

To further characterize the SC-II phase, we tentatively probe the information about Fermi surface under pressure by measuring the Hall effect in the normal state just above T_c. Figure 4(a) shows the in-plane Hall resistivity $\rho_{xy}(H)$ at 50 K for different pressures up to 6 GPa. All $\rho_{xy}(H)$ exhibit a linear behavior with a negative slope, which confirms that the electron-type carriers dominate transport properties of the SC-II phase. In addition, the slope of $\rho_{xy}(H)$ decreases gradually with pressure. To quantify this change, we obtained the Hall coefficient $R_H \equiv d\rho_{xy}/dH$ from the linear fitting to $\rho_{xy}(H)$ and plotted the pressure dependence of R_H at 50 K in Fig. 4(b). As can be seen, the magnitude of $|R_H|$ decreases quickly and tends to level off above 6 GPa, in line with the variation of $T_c^{onset}(P)$ of SC-II shown in Fig. 3. By assuming a simple one-band contribution, the electron-type carrier concentration

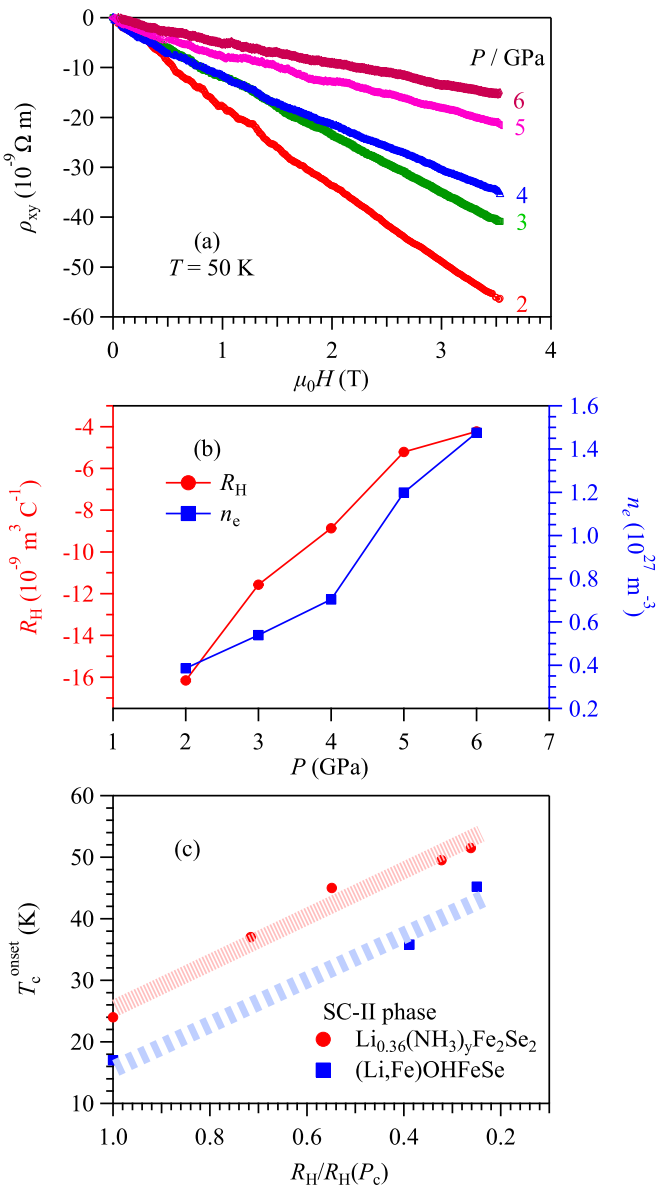

FIG. 4. (a) The Hall resistivity $\rho_{xy}(H)$ at the normal state just above T_c under various pressures. (b) The Hall coefficient $R_{\rm H}$ and the carrier density n_e are determined from the field derivative of ρ_{xy}, $R_{\rm H} \equiv d\rho_{xy}/dH$ and $n_e = -1/(R_{\rm H}e)$ at each pressure. (c) $T_c^{\rm onset}$ as the dependence of $R_{\rm H}/R_{\rm H}(P_c)$ in the SC-II phase of the $Li_{0.36}(NH_3)_yFe_2Se_2$ and (Li,Fe)OHFeSe single crystals [23].

can be estimated as $n_e = -1/(R_{\rm H}e)$. As shown in Fig. 4(b), n_e takes a value of $\sim 0.39 \times 10^{27}\,{\rm m}^{-3}$ at 2 GPa and experiences fourfold enhancements to $\sim 1.5 \times 10^{27}\,{\rm m}^{-3}$ at 6 GPa, tracking nicely the variation of $T_c^{\rm onset}(P)$. It should be noted that the carrier density at 6 GPa is slightly higher than that of $1.3 \times 10^{27}\,{\rm m}^{-3}$ at ambient pressure [24]. We have observed a similar concomitant enhancement of n_e and T_c in the SC-II phase of $(Li_{1-x}Fe_x)OHFeSe$ [23], thus implying a common mechanism controlling the T_c of SC-II phase in these HED FeSe-derived materials. As illustrated in Fig. 4(c), $T_c^{\rm onset}$ of the SC-II phases for both compounds indeed scales linearly with the inverse Hall coefficient $R_{\rm H}/R_{\rm H}(P_c)$ or the electron charge-density n_e, similar to the well-known Uemura's law [29]. In addition, these two curves are nearly parallel with each other, further elaborating a common origin for the SC-II phase. It should be noted that despite the dramatic enhancement of carrier density the relatively small resistivity change above 2 GPa should be caused by the decrease of mobility under pressure.

As mentioned above, the electron doping plays an essential role to raise the T_c of bulk FeSe, giving rise to a variety of HED FeSe-derived bulk materials with an optimal T_c reaching $\sim$46 K at ambient pressure. The observed antiferromagnetic insulating behavior in the overdoped regime suggests the presence of some threshold for band filling to approach the Mott transition [18,30]. This sets an upper limit of T_c for these HED FeSe bulk materials at ambient pressure if the band-structure or Fermi-surface topology remains intact under pressure. Then, high pressure usually broadens the bandwidth, reduces the effective density of states at the Fermi level, and leads to a gradual reduction of T_c as seen in the SC-I phase.

Since the structural transition has been excluded around P_c in (Li,Fe)OHFeSe [23] and is unlikely to occur at such a low pressure of 2 GPa in $Li_{0.36}(NH_3)_yFe_2Se_2$ [31], the sudden reversal of $T_c(P)$ above P_c and the emergence of SC-II should be ascribed to an electronic origin, presumably associated with a Fermi-surface reconstruction. The observed higher carrier concentration in SC-II than that of SC-I, e.g., $1.5 \times 10^{27}{\rm m}^{-3}$ at 6 GPa versus $1.3 \times 10^{27}{\rm m}^{-3}$ at ambient pressure [24], indicates that the band structure of SC-II would allow for more band filling before reaching the Mott transition. It is likely that the Fermi-surface volume is enlarged above P_c. According to a recent ARPES study on FeSe films by Phan *et al.* [32], a compression strain realized in $FeSe/CaF_2$ will enlarge significantly both hole and electron Fermi surfaces in comparison with the strain-free FeSe. Similarly, in these HED FeSe materials, there may exist a critical P_c above which the compression on the FeSe plane can result in a sudden Fermi-surface reconstruction or Lifshitz transition leading to a larger Fermi-surface volume. The Se-Fe-Se angles and the anion height that can be tuned by pressure should be the key factors governing such a transition [33]. In addition, the observed concomitant enhancement of T_c and n_e in SC-II suggests that the Fermi-surface topology in the SC-II phase allows for above P_c a gradual recovery of the density of states that has been reduced in the SC-I phase. It is interesting to note that the two-dome-shaped superconducting phases have been observed in the overdoped $LaFeAsO_{1-x}H_x$ ($0 \leqslant x \leqslant 0.53$) [34] and $LaFeAsO_{1-x}F_x$ ($0 \leqslant x \leqslant 0.75$) [35] at ambient pressure. The two superconducting phases were found to be adjacent with two distinct antiferromagnetically ordered states in $LaFeAsO_{1-x}H_x$ [36], whereas the dome of the SC-II phase in $LaFeAsO_{1-x}F_x$ was confirmed to connect with a $C4$ rotation symmetry-breaking structural transition without low-energy magnetic fluctuations [35]. Further studies are needed to check whether pressure-induced SC-II phase is adjacent to an ordered state in these HED FeSe materials.

Theoretical investigations on the $A_xFe_{2-y}Se_2$ systems have proposed that the observed two superconducting phases under pressure may have different pairing symmetries associated with a renormalization of Fermi-surface topology [37]. Although much endeavor is needed to figure out the underlying

mechanisms, our present study together with those previous high-pressure studies demonstrate that these HED FeSe-derived materials would universally emerge a pressure-induced SC-II phase with the maximum T_c about 10 K higher than that of the SC-I phase [20,22,23]. This offers an alternative route to further raise the T_c of these HED FeSe-derived materials.

To summarize, we have performed the magnetotransport measurements on a $Li_{0.36}(NH_3)_yFe_2Se_2$ single crystal under hydrostatic pressure up to 12 GPa and constructed the *T*-*P* phase diagram featured by the emergence of an SC-II phase above $P_c \approx 2$ GPa. We have achieved the highest $T_c^{\text{onset}} \approx 55$ K above 10 GPa among the FeSe-based bulk materials. In addition, we obtained a nearly parallel scaling behavior between T_c^{onset} and the inverse Hall coefficient for the SC-II phase of both $Li_{0.36}(NH_3)_yFe_2Se_2$ and (Li,Fe)OHFeSe. Our present study thus demonstrates a way for high pressure to further raise T_c of these HED FeSe-based materials by increasing the effective charge-carrier concentration via a possible Fermi-surface reconstruction at P_c.

This work was supported by the National Science Foundation of China (Grants No. 11574377, No. 11574394, and No. 11774423), the National Basic Research Program of China (Grant No. 2014CB921500), the National Key R&D Program of China (Grant No. 2016YFA0300504), the Strategic Priority Research Program and Key Research Program of Frontier Sciences of the Chinese Academy of Sciences (Grants No. QYZDB-SSW-SLH013 and No. XDB07020100), the Fundamental Research Funds for the Central Universities, and the Research Funds of Renmin University of China (Grants No. 15XNLF06 and No. 15XNLQ07).

P.S., J.P.S., and S.H.W. contributed equally to this work.

[1] F. C. Hsu, J. Y. Luo, K. W. Yeh, T. K. Chen, T. W. Huang, P. M. Wu, Y. C. Lee, Y. L. Huang, Y. Y. Chu, D. C. Yan, and M. K. Wu, Proc. Natl. Acad. Sci. USA **105**, 14262 (2008).

[2] J. G. Guo, S. F. Jin, G. Wang, S. C. Wang, K. X. Zhu, T. T. Zhou, M. He, and X. L. Chen, Phys. Rev. B **82**, 180520(R) (2010).

[3] X. F. Lu, N. Z. Wang, H. Wu, Y. P. Wu, D. Zhao, X. Z. Zeng, X. G. Luo, T. Wu, W. Bao, G. H. Zhang, F. Q. Huang, Q. Z. Huang, and X. H. Chen, Nature Mater. **14**, 325 (2015).

[4] E. W. Scheidt, V. R. Hathwar, D. Schmitz, A. Dunbar, W. Scherer, F. Mayr, V. Tsurkan, J. Deisenhofer, and A. Loidl, Eur. Phys. J. B **85**, 279 (2012).

[5] X. Dong, K. Jin, D. Yuan, H. Zhou, J. Yuan, Y. Huang, W. Hua, J. Sun, P. Zheng, W. Hu, Y. Mao, M. Ma, G. Zhang, F. Zhou, and Z. Zhao, Phys. Rev. B **92**, 064515 (2015).

[6] B. Lei, J. H. Cui, Z. J. Xiang, C. Shang, N. Z. Wang, G. J. Ye, X. G. Luo, T. Wu, Z. Sun, and X. H. Chen, Phys. Rev. Lett. **116**, 077002 (2016).

[7] H.-D. Wang, C.-H. Dong, Z.-J. Li, Q.-H. Mao, S.-S. Zhu, C.-M. Feng, H. Q. Yuan, and M.-H. Fang, Europhys. Lett. **93**, 47004 (2011).

[8] Q.-Y. Wang, Z. Li, W.-H. Zhang, Z.-C. Zhang, J.-S. Zhang, W. Li, H. Ding, Y.-B. Ou, P. Deng, K. Chang, J. Wen, C.-L. Song, K. He, J.-F. Jia, S.-H. Ji, Y.-Y. Wang, L.-L. Wang, X. Chen, X.-C. Ma, and Q.-K. Xue, Chin. Phys. Lett. **29**, 037402 (2012).

[9] J. F. Ge, Z. L. Liu, C. Liu, C. L. Gao, D. Qian, Q. K. Xue, Y. Liu, and J. F. Jia, Nature Mater. **14**, 285 (2015).

[10] X. Dong, H. Zhou, H. Yang, J. Yuan, K. Jin, F. Zhou, D. Yuan, L. Wei, J. Li, X. Wang, G. Zhang, and Z. Zhao, J. Am. Chem. Soc. **137**, 66 (2015).

[11] H. Lin, J. Xing, X. Zhu, H. Yang, and H.-H. Wen, Sci. China: Phys., Mech. Astron. **59**, 657404 (2016).

[12] C. L. Song, H. M. Zhang, Y. Zhong, X. P. Hu, S. H. Ji, L. Wang, K. He, X. C. Ma, and Q. K. Xue, Phys. Rev. Lett. **116**, 157001 (2016).

[13] X. Shi, Z. Q. Han, X. L. Peng, P. Richard, T. Qian, X. X. Wu, M. W. Qiu, S. C. Wang, J. P. Hu, Y. J. Sun, and H. Ding, Nat. Commun. **8**, 14988 (2017).

[14] B. Lei, N. Z. Wang, C. Shang, F. B. Meng, L. K. Ma, X. G. Luo, T. Wu, Z. Sun, Y. Wang, Z. Jiang, B. H. Mao, Z. Liu, Y. J. Yu, Y. B. Zhang, and X. H. Chen, Phys. Rev. B **95**, 020503(R) (2017).

[15] L. Zhao, A. Liang, D. Yuan, Y. Hu, D. Liu, J. Huang, S. He, B. Shen, Y. Xu, X. Liu, L. Yu, G. Liu, H. Zhou, Y. Huang, X. Dong, F. Zhou, K. Liu, Z. Lu, Z. Zhao, C. Chen, Z. Xu, and X. J. Zhou, Nat. Commun. **7**, 10608 (2016).

[16] Y. J. Yan, W. H. Zhang, M. Q. Ren, X. Liu, X. F. Lu, N. Z. Wang, X. H. Niu, Q. Fan, J. Miao, R. Tao, B. P. Xie, X. H. Chen, T. Zhang, and D. L. Feng, Phys. Rev. B **94**, 134502 (2016).

[17] T. Qian, X. P. Wang, W. C. Jin, P. Zhang, P. Richard, G. Xu, X. Dai, Z. Fang, J. G. Guo, X. L. Chen, and H. Ding, Phys. Rev. Lett. **106**, 187001 (2011).

[18] B. Lei, Z. J. Xiang, X. F. Lu, N. Z. Wang, J. R. Chang, C. Shang, A. M. Zhang, Q. M. Zhang, X. G. Luo, T. Wu, Z. Sun, and X. H. Chen, Phys. Rev. B **93**, 060501 (2016).

[19] M. Q. Ren, Y. J. Yan, X. H. Niu, R. Tao, D. Hu, R. Peng, B. P. Xie, J. Zhao, T. Zhang, and D. L. Feng, Sci. Adv. **3**, e1603238 (2017).

[20] L. Sun, X. J. Chen, J. Guo, P. Gao, Q. Z. Huang, H. Wang, M. Fang, X. Chen, G. Chen, Q. Wu, C. Zhang, D. Gu, X. Dong, L. Wang, K. Yang, A. Li, X. Dai, H. K. Mao, and Z. Zhao, Nature (London) **483**, 67 (2012).

[21] H. Fujita, T. Kagayama, K. Shimizu, Y. Yamamoto, J. I. Mizuki, H. Okazaki, and Y. Takano, J. Phys.: Conf. Ser. **592**, 012070 (2015).

[22] M. Izumi, L. Zheng, Y. Sakai, H. Goto, M. Sakata, Y. Nakamoto, H. L. Nguyen, T. Kagayama, K. Shimizu, S. Araki, T. C. Kobayashi, T. Kambe, D. Gu, J. Guo, J. Liu, Y. Li, L. Sun, K. Prassides, and Y. Kubozono, Sci. Rep. **5**, 9477 (2015).

[23] J. P. Sun, P. Shahi, H. X. Zhou, Y. L. Huang, K. Y. Chen, B. S. Wang, S. L. Ni, N. N. Li, K. Zhang, W. G. Yang, Y. Uwatoko, K. Jin, F. Zhou, D. Singh, X. L. Dong, Z. X. Zhao, and J.-G. Cheng, Nat. Commun. (2018) (to be published).

[24] S. Sun, S. Wang, R. Yu, and H. Lei, Phys. Rev. B **96**, 064512 (2017).

[25] J. G. Cheng, K. Matsubayashi, S. Nagasaki, A. Hisada, T. Hirayama, M. Hedo, H. Kagi, and Y. Uwatoko, Rev. Sci. Instrum. **85**, 093907 (2014).

[26] J. P. Sun, K. Matsuura, G. Z. Ye, Y. Mizukami, M. Shimozawa, K. Matsubayashi, M. Yamashita, T. Watashige, S. Kasahara, Y. Matsuda, J. Q. Yan, B. C. Sales, Y. Uwatoko, J. G. Cheng, and T. Shibauchi, Nat. Commun. **7**, 12146 (2016).

[27] S. Klotz, K. Takemura, T. Strassle, and T. Hansen, J. Phys.: Condens. Matter **24**, 325103 (2012).

[28] Z. A. Ren, W. Lu, J. Yang, W. Yi, X. L. Shen, Z. C. Li, G. C. Che, X. L. Dong, L. L. Sun, F. Zhou, and Z. X. Zhao, Chin. Phys. Lett. **25**, 2215 (2008).

[29] Y. J. Uemura, G. M. Luke, B. J. Sternlieb, J. H. Brewer, J. F. Carolan, W. N. Hardy, R. Kadono, J. R. Kempton, R. F. Kiefl, S. R. Kreitzman, P. Mulhern, T. M. Riseman, D. L. Williams, B. X. Yang, S. Uchida, H. Takagi, J. Gopalakrishnan, A. W. Sleight, M. A. Subramanian, C. L. Chien, M. Z. Cieplak, G. Xiao, V. Y. Lee, B. W. Statt, C. E. Stronach, W. J. Kossler, and X. H. Yu, Phys. Rev. Lett. **62**, 2317 (1989).

[30] P. A. Lee, N. Nagaosa, and X.-G. Wen, Rev. Mod. Phys. **78**, 17 (2006).

[31] We have attemptted to measure the high-pressure synchrotron x-ray powder diffration on $Li_{0.36}(NH_3)_yFe_2Se_2$, but our effort was hampered by the fact that the intercalated ammonia easily escapes during the sample preparation.

[32] G. N. Phan, K. Nakayama, K. Sugawara, T. Sato, T. Urata, Y. Tanabe, K. Tanigaki, F. Nabeshima, Y. Imai, A. Maeda, and T. Takahashi, Phys. Rev. B **95**, 224507 (2017).

[33] S. Mandal, P. Zhang, S. Ismail-Beigi, and K. Haule, Phys. Rev. Lett. **119**, 067004 (2017).

[34] S. Iimura, S. Matsuishi, H. Sato, T. Hanna, Y. Muraba, S. W. Kim, J. E. Kim, M. Takata, and H. Hosono, Nat. Commun. **3**, 943 (2012).

[35] J. Yang, R. Zhou, L. L. Wei, H. X. Yang, J. Q. Li, Z. X. Zhao, and G. Q. Zheng, Chin. Phys. Lett. **32**, 107401 (2015).

[36] M. Hiraishi, S. Iimura, K. M. Kojima, J. Yamaura, H. Hiraka, K. Ikeda, P. Miao, Y. Ishikawa, S. Torii, M. Miyazaki, I. Yamauchi, A. Koda, K. Ishii, M. Yoshida, J. Mizuki, R. Kadono, R. Kumai, T. Kamiyama, T. Otomo, Y. Murakami, S. Matsuishi, and H. Hosono, Nat. Phys. **10**, 300 (2014).

[37] T. Das and A. V. Balatsky, New J. Phys. **15**, 093045 (2013).